Analysis of the viscous/molecular subgrid-scale dissipation terms in LES based on transport equations: a-priori tests

Sara Tavares Rego

September 2008

Abstract

Some subgrid modelling strategies in large eddy simulations (LES) involve the use of a transport equation for the subgrid-scale (SGS) kinetic energy. Likewise, for problems regarding active or passive scalar fields, a SGS scalar variance transport equation is also used. The terms from these transport equations comprise sub-filter scale quantities that are not accessible during LES and thus require modelling. Our main focus here concerns the modelling the viscous and the molecular SGS dissipation terms, for which three strategies are assessed. The models assessed here are (a) the classical model (Schumann (1975) [1], Yoshizawa (1982) [2]), (b) the model used in hybrid RANS/LES (Paterson and Peltier (2005) [3], Hanjalic (2005) [4]), and (c) the model for the molecular SGS dissipation of SGS scalar variance from Jiménez *et al.* (2001) [5]. *A priori* tests are performed to the data bank results from direct numerical simulations of statistically stationary homogeneous isotropic turbulence (da Silva and Pereira (2007) [6]) and the behaviour of these models is interpreted by means of statistical analysis and spectra from the exact and modelled molecular SGS dissipations. Both classical models for the molecular SGS dissipation and the model from Jiménez *et al.* for the molecular SGS dissipation of SGS scalar variance yield very good results, whereas the models tested here and used in hybrid RANS/LES give poor results.

Keywords: Subgrid-scale modelling, Viscous/molecular SGS dissipation, Isotropic turbulence, Direct Numerical Simulations

1 Introduction

In large-eddy simulations (LES) the large flow structures which are responsible for the most important transfers of mass, momentum and heat are explicitly calculated while the effect of the small scales is modelled by a subgrid-scale (SGS) model. In many flow simulations the small scales of motion are statistically close to isotropic, carry a relatively small amount of the total kinetic energy, adjust almost immediately to the dynamics of the large scales, and their major role is associated with the viscous dissipation of kinetic energy. These facts allowed the development of relatively simple SGS models possessing some degree of Universality which makes them very attractive compared to other modelling strategies *e.g.* based on the Reynolds averaged Navier-Stokes equations - RANS (see [7, 8] for a review of LES).

However, it has been recognised early on that in some engineering and Natural flows the design of Universal and simple SGS models would be difficult to achieve for a number of reasons: (*i*) the isotropic assumption of the small scale motions is not observed in many flows even at very high Reynolds numbers, particularly for the passive scalar field [9, 10], (*ii*) in many LES the SGS motions do possess a significant part of the total kinetic energy [11] and, closely related to this, (*iii*) for high Reynolds numbers and/or coarse meshes the SGS motions need a non-negligible time to adjust to local unsteadiness from the large scales *i.e.* the *local equilibrium assumption* between the large and small scales of motion fails [12, 13].

In order to overcome these limitations numerous SGS models use a transport equation for the SGS kinetic energy [1, 2, 14, 15, 16, 17, 18, 19, 20, 21]. The use of a transport equation for the SGS kinetic energy is interesting also to many hybrid RANS/LES and URANS/LES modelling strategies *e.g.* [22, 23, 24, 25, 26].

Similarly, in LES involving a passive or active scalar field several new unclosed terms arise. One way to deal with these unknown terms is to solve an additional SGS scalar variance transport equation [27]. For example, in LES of reacting flows the variance of the mixture fraction is very important [28]. Therefore, some combustion models use an additional transport equation for the variance of the SGS mixture fraction *e.g.* [5, 29, 30].

By far the greatest challenge when modelling the transport equations for the SGS kinetic energy and SGS scalar variance comes from the *viscous/molecular SGS dissipation* terms which represent the final dissipation of SGS kinetic energy and SGS scalar variance caused by viscous/molecular effects, at the end of the energy cascade mechanism. Compared to the viscous dissipation of (total) kinetic energy and the molecular dissipation of (total) scalar variance for which much work was already undertaken (*e.g.* [31, 32, 33, 34, 35]) few works analysed the viscous/molecular SGS dissipation terms. For the SGS kinetic energy equation the viscous SGS dissipation term was analysed by Meneveau and O'Neil [36], Menon *et al.* [37], da Silva and Métais [12], and Chumakov [38]. Much less is known about the molecular SGS dissipation of the SGS scalar variance, although some works analysed a related quantity - the sub-filter scalar dissipation - due to its importance to combustion simulations ([39, 40, 29]).

The classical models used for the molecular SGS dissipation terms are based in the *self-similarity* of the *energy cascade*, but some new models have been proposed recently. For the SGS kinetic energy equation new models for the viscous SGS dissipation term were developed by Langhe *et al.* [24], Chaouat and Schiestel [41], and Chumakov and Rutland [42]. Concerning the SGS scalar variance equation Jiménez *et al.* [5, 30], and Chumakov and Rutland [42, 43] proposed new models for the molecular SGS dissipation term.

The goal of the present work is to assess the performance of several models in *a-priori* tests. It is expected that the present analysis will highlight the strengths and limitations of the present models, and will give new insights which will help the development of more accurate models for the viscous/molecular SGS dissipation terms. The analysis carried out here is made by applying a box filter to direct numerical simulations (DNS) of statistically stationary (forced) homogeneous isotropic turbulence [6] using correlation coefficients, joint probability density functions (PDFs), several one point statistics such as the variance, skewness, and the flatness factors, as well as spectra from the exact and modelled viscous/molecular SGS dissipations. Even if the models analysed here are to be used in much more complex turbulent flows than in isotropic turbulence, they have to show good results in this simple flow if they are to succeed in more complex situations.

This article is organised as follows. In the next section the equations governing the exact and modelled SGS kinetic energy and SGS scalar variance and each one of its terms are described. The classical as well as new models used for the viscous/molecular SGS dissipation terms are reviewed. In section 3 we describe the DNS of isotropic turbulence used in this work. Section 4 analyses the performance of the some models using classical *a priori* tests. Finally, in section 5 the article ends with an overview of the main results, conclusions, and perspectives for modelling the viscous/molecular SGS dissipation terms.

2 Governing equations

In this section we review the exact and modelled transport equations for the SGS kinetic energy and SGS scalar variance. The models currently used for the viscous/molecular SGS dissipation terms are reviewed.

2.1 Evolution of the SGS kinetic energy

The SGS kinetic energy $\tau_{ii}/2$ is governed by the exact equation see *e.g* [6, 12, 44],

$$\frac{D}{Dt}\left(\frac{\tau_{ii}}{2}\right) = \underbrace{\frac{1}{2}\frac{\partial}{\partial x_j}\left[\overline{u_i u_i}\ \overline{u_j} - \overline{u_i u_i u_j}\right]}_{D_{turb}} + \underbrace{\frac{\partial}{\partial x_j}\left[\overline{p}\ \overline{u_j} - \overline{p u_j}\right]}_{D_{press}}$$
$$+ \underbrace{\nu\frac{\partial^2}{\partial x_j \partial x_j}\left(\frac{\tau_{ii}}{2}\right)}_{D_{visc}} - \underbrace{\nu\left[\overline{\frac{\partial u_i}{\partial x_j}\frac{\partial u_i}{\partial x_j}} - \frac{\partial \overline{u_i}}{\partial x_j}\frac{\partial \overline{u_i}}{\partial x_j}\right]}_{\Sigma} + \underbrace{\frac{\partial}{\partial x_j}\left(\tau_{ij}\overline{u_i}\right)}_{D_{gs/sgs}} - \underbrace{\tau_{ij}\frac{\partial \overline{u_i}}{\partial x_j}}_{P}, \tag{1}$$

where u_i is the velocity vector field, $\tau_{ij} = \overline{u_i u_j} - \overline{u_i}\ \overline{u_j}$ is the SGS stresses tensor, ν is the molecular viscosity, and the overlay symbol $(\overline{\ })$ represents a spatial filtering operation. Note that here $\overline{p}$ means $\frac{\overline{p}}{\rho}$ for convenience, where p is the pressure field.

In equation (1) D_{turb}, D_{press} and D_{visc} represent the diffusion of SGS kinetic energy through SGS turbulent fluctuations, pressure-velocity interactions, and molecular viscosity, respectively. The final dissipation of SGS energy by molecular viscosity, associated with the "end" of the energy cascade mechanism, is represented by term Σ - *the viscous SGS dissipation* term. The two last terms in equation (1) appear also (with opposite sign) in the grid-scale (GS) kinetic energy equation $\overline{K} = (\overline{u_i})^2/2$, and thus represent exchanges between the GS and SGS kinetic energy equations. Term $D_{gs/sgs}$ - GS/SGS diffusion - represents a redistribution due to GS/SGS interactions whereas P - GS/SGS transfer - represents the net transfer of kinetic energy between GS and SGS. If $P > 0$ the term acts as a source in equation (1) and describes the flow of energy from GS into SGS (forward scatter). Backscatter occurs whenever $P < 0$.

2.2 Evolution of the SGS scalar variance

The exact equation for the evolution of the SGS scalar variance, $q_\theta/2 = [\overline{\theta^2} - \overline{\theta}^2]/2$, is given by (Jiménez *et al.* [5, 30]),

$$\frac{D}{Dt}\left(\frac{q_\theta}{2}\right) = \underbrace{\frac{1}{2}\frac{\partial}{\partial x_j}\left[\overline{\theta^2}\ \overline{u_j} - \overline{\theta^2 u_j}\right]}_{D_{\theta turb}} + \underbrace{\gamma\frac{\partial^2}{\partial x_j \partial x_j}\left(\frac{q_\theta}{2}\right)}_{D_{\theta molec}}$$
$$\underbrace{-\gamma\left[\overline{G_j G_j} - \overline{G_j}\ \overline{G_j}\right]}_{\Sigma_\theta} + \underbrace{\frac{\partial}{\partial x_j}\left(q_j\overline{\theta}\right)}_{D_{\theta gs/sgs}} - \underbrace{q_j\overline{G_j}}_{P_\theta} \tag{2}$$

where $q_j = \overline{\theta u_j} - \overline{\theta}\ \overline{u_j}$ represents the SGS scalar fluxes, $\overline{G_j} = \partial\overline{\theta}/\partial x_j$ is the filtered scalar gradient, and γ is the molecular diffusivity.

In equation (2) terms $D_{\theta turb}$, $D_{\theta molec}$ and $D_{\theta gs/sgs}$ represent the diffusion due to SGS motions, molecular diffusivity and scalar GS/SGS interactions, respectively. The term Σ_θ is the *molecular SGS dissipation* and represents the molecular dissipation of SGS scalar variance, while P_θ is the net transfer from the GS scalar variance, $\overline{\Theta} = (\overline{\theta})^2/2$ (see Kang and Meneveau [45], Jiménez *et al.* [30]). Notice that for cut-off filters the SGS kinetic energy is equal to $\tau_{ii}/2 = \overline{u_i''\ u_i''}/2$, where u_i'' is the subgrid-scale part of the velocity vector, while the SGS scalar variance becomes $q_\theta/2 = (\overline{\theta''^2})/2$.

2.3 Modelled equations for the SGS kinetic energy and SGS scalar variance

The SGS kinetic energy transport equation is usually modelled replacing equation (1) by [18, 20],

$$\frac{\partial}{\partial t}\left(K_{sgs}\right) + \frac{\partial}{\partial x_j}\left(K_{sgs}\overline{u_j}\right) = D^\Delta + P^\Delta - \varepsilon^\Delta. \tag{3}$$

where K_{sgs} is the modelled SGS kinetic energy $\tau_{ii}/2$, and the convective term in the lhs of the equation is written in conservative form. D^Δ represents the sum of the diffusion terms from equation (1) D_{turb}, D_{press}, D_{visc}, and $D_{gs/sgs}$. The second term on the rhs of equation (3) is the modelled SGS energy production, $P^\Delta = -\tau_{ij}\partial\overline{u_i}/\partial x_j$, and ε^Δ is the modelled viscous SGS dissipation corresponding to term Σ in equation (1).

For the SGS scalar variance the model equation is [14],

$$\frac{\partial}{\partial t}\left(\Theta_{sgs}\right) + \frac{\partial}{\partial x_j}\left(\Theta_{sgs}\overline{u_j}\right) = D_\theta^\Delta + P_\theta^\Delta - \varepsilon_\theta^\Delta, \tag{4}$$

where Θ_{sgs} is the modelled SGS scalar variance $q_\theta/2$, and the terms on the right hand side of equation (4) account for the diffusion terms in equation (2) $D_{\theta turb}$, $D_{\theta press}$ and $D_{\theta molec}$, the production term P_θ, and the molecular SGS dissipation Σ_θ, respectively.

2.4 Modelling the viscous/molecular SGS dissipation terms

Arguably, the biggest challenge for modelling in equations (3) and (4) comes from the viscous and molecular dissipation of SGS kinetic energy and SGS scalar variance, respectively, represented by terms ε^{Δ} and $\varepsilon_{\theta}^{\Delta}$.

The classical modelling used for ε^{Δ} and $\varepsilon_{\theta}^{\Delta}$ is based on the *self-similarity of the energy cascade* and on the *dissipation law* [46]. Supposing that at the subgrid-scale level the characteristic velocity and length scales are the square root of the SGS kinetic energy $u \sim K_{sgs}^{1/2}$, and the implicit filter width $l \sim \Delta$, respectively, we obtain the classical model for ε^{Δ} [1, 2, 17, 18, 20],

$$\varepsilon_{a}^{\Delta} = C_{\varepsilon}^{a} \frac{K_{sgs}^{3/2}}{\Delta}, \tag{5}$$

whereas for the SGS scalar variance equation the dissipation term is modelled by [14],

$$\varepsilon_{\theta a}^{\Delta} = C_{\varepsilon\theta}^{a} \frac{K_{sgs}^{1/2} \Theta_{sgs}}{\Delta}. \tag{6}$$

where C_{ε}^{a} and $C_{\varepsilon\theta}^{a}$ are model constants. Considering an inertial range kinetic energy spectrum and an inertial-convective range scalar variance spectrum, the definitions of the subgrid-scale kinetic energy and of the subgrid-scale scalar variance, together with equations (5) and (6), lead to the following expressions for the model constants C_{ε}^{a} and $C_{\varepsilon\theta}^{a}$, [1, 14],

$$C_{\varepsilon}^{a} = \pi \left(\frac{2}{3 C_{K}} \right)^{3/2} \tag{7}$$

and,

$$C_{\varepsilon\theta}^{a} = \frac{2\pi}{3 C_{\theta K}} \left(\frac{2}{3 C_{K}} \right)^{1/2}, \tag{8}$$

where C_{K} and $C_{\theta K}$ are the Kolmogorov and Obukhov-Corrsin constants, respectively, and the implicit grid filter Δ is taken from the inertial and inertial-convective range, where $\langle \varepsilon \rangle = \langle \varepsilon_{a}^{\Delta} \rangle$, and $\langle \varepsilon_{\theta} \rangle = \langle \varepsilon_{\theta a}^{\Delta} \rangle$. Using $C_{K} = 1.6$ and $C_{\theta K} = 1.34$ we get $C_{\varepsilon}^{a} = 0.845$ and $C_{\varepsilon\theta}^{a} = 2.02$, respectively. In most models these model constants are either chosen as constants for the whole flow (*e.g.* [1, 14, 19]), or calculated dynamically (*e.g.* [17, 18, 20]).

New models for ε^{Δ} and $\varepsilon_{\theta}^{\Delta}$ have been proposed recently. In hybrid continuous RANS/LES turbulence modelling it is sometimes advantageous to model the viscous SGS dissipation by replacing K_{sgs} by $\overline{K}$ in equation (5), which leads to the following model for ε^{Δ} [3, 4],

$$\varepsilon_{b}^{\Delta} = C_{\varepsilon}^{b} \frac{\overline{K}^{3/2}}{\Delta}. \tag{9}$$

A similar equation for the molecular SGS dissipation of SGS scalar variance would be,

$$\varepsilon_{\theta b}^{\Delta} = C_{\varepsilon\theta}^{b} \frac{\overline{K}^{1/2} \overline{\Theta}}{\Delta}. \tag{10}$$

These formulations are particularly useful to switch between the RANS and the LES modes in the so-called detached-eddy simulations (DES).

Some models are based on the SGS mechanical-to-thermal time scale ratio

$$r_{sgs} = \frac{K_{sgs}/\varepsilon^{\Delta}}{\Theta_{sgs}/\varepsilon_{\theta}^{\Delta}}, \tag{11}$$

which appears as a SGS version of the (total) mechanical-to-thermal time scale ratio defined as,

$$r = \frac{K/\varepsilon}{\Theta/\varepsilon_{\theta}} \tag{12}$$

where $K = (u_i)^2/$ is the (total) kinetic energy and $\Theta = \theta^2/2$ is the (total) scalar variance. Note that there is now substantial evidence that, at least the mechanical-to-thermal time scale ratio defined in

equation (12) is not Universal as attested by Overholt and Pope [32] in numerical simulations of isotropic turbulence.

In LES involving turbulent combustion some authors prefer to model the "sub-filter scalar dissipation" term defined by $\gamma\overline{G_j G_j}$ since the term $\gamma\overline{G_j}\ \overline{G_j}$ in the definition of Σ_θ can be obtained explicitly from the filtered scalar fields [5, 29, 39, 40]. In particular Jiménez *et al.* [5] derived a new model for the sub-filter scalar dissipation based in equation (11), and on the Smagorinsky [47] and the Yoshizawa [48] models. The model equation is,

$$\gamma\overline{G_j G_j} = \frac{C_\theta^c}{2}\left(\frac{\Theta_{sgs}}{K_{sgs}}\right)\overline{\frac{\partial u_i}{\partial x_j}\frac{\partial u_i}{\partial x_j}}. \tag{13}$$

Tests in isotropic turbulence suggest that the model constant is approximately equal to $C_\theta^c \sim 1/Sc$. A similar model for the molecular SGS dissipation $\varepsilon_\theta^\Delta$ would be given by,

$$\varepsilon_{\theta c}^\Delta = \frac{C_\theta^c}{2}\left(\frac{\Theta_{sgs}}{K_{sgs}}\right)\varepsilon^\Delta. \tag{14}$$

3 Direct numerical simulations of isotropic turbulence

3.1 Numerical code and data bank description

The numerical code used in the present simulations is a standard pseudo-spectral code in which the temporal advancement is made with an explicit 3^{rd} order Runge-Kutta scheme. The physical domain consists in a periodic box of sides 2π and the simulations were fully dealiased using the 3/2 rule. Both the velocity and scalar large scales were forced in order to sustain the turbulence using the method described by Alvelius [49]. The same code was recently used by da Silva and Pereira [6, 13].

Three DNS of statistically steady (forced) homogeneous isotropic turbulence using $N = 192$ collocation points in each direction were carried out. The Taylor based Reynolds number and Schmidt numbers for the three simulations are equal to $Re_\lambda = 95.6$ and $Sc = 0.7$; $Re_\lambda = 95.6$ and $Sc = 0.2$; and $Re_\lambda = 39.4$ and $Sc = 3.0$, respectively. The ratio between the box size and the integral scale is $L/L_{11} > 4$ and we have $k_{max}\eta > 1.5$ and $k_{max}\eta_B > 1.5$ in all simulations, where $\eta = (\nu^3/\varepsilon)^{1/4}$ and $\eta_B = \eta/Sc^{1/2}$ are the Kolmogorov and Batchelor micro-scales, respectively. For the case $Re_\lambda = 95.6$ and $Sc = 0.7$ the velocity and scalar spectra display a $-5/3$ range which shows the existence of an inertial range region. Full details are given in reference [6].

The separation between grid and subgrid-scales was made using a spatial filtering operation defined by the integral,

$$\overline{\phi}(\vec{x}) = \int_{-\Delta/2}^{+\Delta/2}\int_{-\Delta/2}^{+\Delta/2}\int_{-\Delta/2}^{+\Delta/2}\phi(\vec{x}')G_\Delta(\vec{x}-\vec{x}')d\vec{x}', \tag{15}$$

where $\overline{\phi}(\vec{x})$ represents the spatially filtered variable $\phi(\vec{x})$, and $G_\Delta(\vec{x})$ is the filter kernel. Only box filtering is used in this work, whose filter kernel is defined by

$$G_\Delta(\vec{x}-\vec{\xi}) = \begin{cases} \frac{1}{\Delta} & \text{if } |\vec{x}-\vec{\xi}| < \frac{\Delta}{2} \\ 0 & \text{otherwise} \end{cases}$$

Four different filter widths were used with $\Delta_m = m\Delta x$, with $m = 2, 4, 8, 16$. Their location in the energy and scalar variance spectrum is shown in reference [6], where one can see that the implicit cut-off wave number for the filter with $\Delta/\Delta x = 16$ is within the inertial range region.

4 Assessment of models for the viscous/molecular dissipation of SGS kinetic energy and SGS scalar gradient, ε^Δ and $\varepsilon_\theta^\Delta$

The exact or 'real' viscous/molecular dissipations of SGS kinetic energy and SGS scalar variance are defined in equations (1) and (2), respectively, while we denote by ε_m^Δ and $\varepsilon_{\theta m}^\Delta$ the modelled values of these quantities using a given model m. Three models were analysed here which we denote by $m = a, b, c$. The symbol $m = a$ represents the classical models defined in equations (5) and (6). The new models used in hybrid RANS/LES defined by equations (9) and (10) are denoted by $m = b$. Finally, we analyse also the model proposed by Jiménez *et al.* [5] for the molecular dissipation of SGS scalar variance $\varepsilon_{\theta c}^\Delta$.

All the *a priori* tests carried out here were made with the data in the LES grid. The results were obtained using several (10) instantaneous fields from the three DNS described before and used also in da Silva and Pereira [6, 13] *i.e.* with (i) $\mathsf{Re}_\lambda = 39.4$ and $\mathsf{Sc} = 3.0$, (ii) $\mathsf{Re}_\lambda = 95.6$ and $\mathsf{Sc} = 0.7$ and, (iii) $\mathsf{Re}_\lambda = 95.6$ and $\mathsf{Sc} = 0.2$. Moreover, note that in order to conduct the *a priori* tests the constants appearing in the equations defining each model *e.g.* equations (5) and (6) for the classical model, were set to $C_\varepsilon^a = 1$ and $C_{\varepsilon\theta}^a = 1$, respectively, before being evaluated from the data.

4.1 Analysis of the classical models ε_a^Δ and $\varepsilon_{\theta a}^\Delta$

Figure 1 shows the correlation coefficients between the exact and the modelled viscous/molecular SGS dissipations - $\mathsf{Corr}(\Sigma, \varepsilon_a^\Delta)$ and $\mathsf{Corr}(\Sigma_\theta, \varepsilon_{\theta a}^\Delta)$. For small filter sizes, characteristic of the dissipative

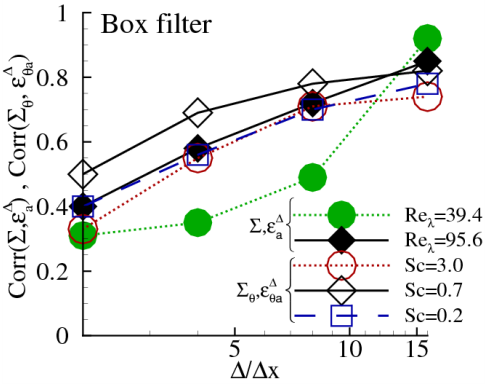

Figure 1: Correlation coefficients between the exact molecular SGS dissipations (Σ and Σ_θ) and their classical models (ε_a^Δ and $\varepsilon_{\theta a}^\Delta$) defined by equations (5) and (6). The correlations were obtained with filter widths $\Delta/\Delta x = 2$, 4, 8, and 16, and were computed using the data in the LES mesh.

range, the correlations between Σ and ε_a^Δ, and between Σ_θ and $\varepsilon_{\theta a}^\Delta$ are low or moderate. However, all the correlations increase with the filter size and become actually very high for large *i.e.* inertial range filter sizes. An encouraging result which is apparent from the figure is that the correlations tend to be higher for higher Reynolds numbers. Concerning the scalar field we see here for the first time that the correlation between the exact and modelled molecular SGS dissipation (Σ_θ and $\varepsilon_{\theta a}^\Delta$) is also quite high.

To have a more detailed picture the results described above Figs. 2 (a) and (b) show the joint probability density functions between Σ and ε_a^Δ, and between Σ_θ and $\varepsilon_{\theta a}^\Delta$, for the simulation with $\mathsf{Re}_\lambda = 95.6$ and $\mathsf{Sc} = 0.7$, and filter widths $\Delta/\Delta x = 4$ and $\Delta/\Delta x = 16$. For the smaller filter no correlation can be observed from the shape of the joint PDFs between both Σ and ε_a^Δ, and between Σ_θ and $\varepsilon_{\theta a}^\Delta$. However, in agreement with the correlation coefficients described above, for $\Delta/\Delta x = 16$ one observes a strong correlation between the variables. Similar results were observed for the simulations with $\mathsf{Re}_\lambda = 95.6$ and $\mathsf{Sc} = 0.2$, and for $\mathsf{Re}_\lambda = 39.4$ and $\mathsf{Sc} = 3.0$.

Fig. 3 displays $\langle C_\varepsilon^a \rangle$ and $\langle C_{\varepsilon\theta}^a \rangle$ obtained for all the simulations and filter sizes used in this work. For $\mathsf{Re}_\lambda = 95.6$ and $\mathsf{Sc} = 0.7$ the constant $C_{\varepsilon\theta}^a$ associated with the scalar field displays a slightly larger variation with the filter size than the constant C_ε^a associated with the velocity field. In particular the constant C_ε^a is higher for the smaller Reynolds number case.

Despite its Reynolds and Schmidt number dependence, for the higher Reynolds number case the constants C_ε^a and $C_{\varepsilon\theta}^a$ seem to display an asymptotic behaviour, and tend to the theoretical values as the filter size increases [50].

The results seem to show a linear dependence of $C_{\varepsilon\theta}^\Delta$ from the filter size.

The variance of a given quantity expresses its local "intensity" and therefore is useful in order to characterise the local "activity" of the SGS dissipation terms. The exact and modelled variances (not shown) increase with the filter size, implying that the classical models get the correct trend, which reflects the increasing importance of the molecular SGS dissipation terms when more SGS production - P and P_θ - contribute to it as the filter size increases. The agreement between Σ and ε_a^Δ is quite good, particularly for the lower Reynolds number case. A similar comparison between Σ_θ and $\varepsilon_{\theta a}^\Delta$ shows that the agreement

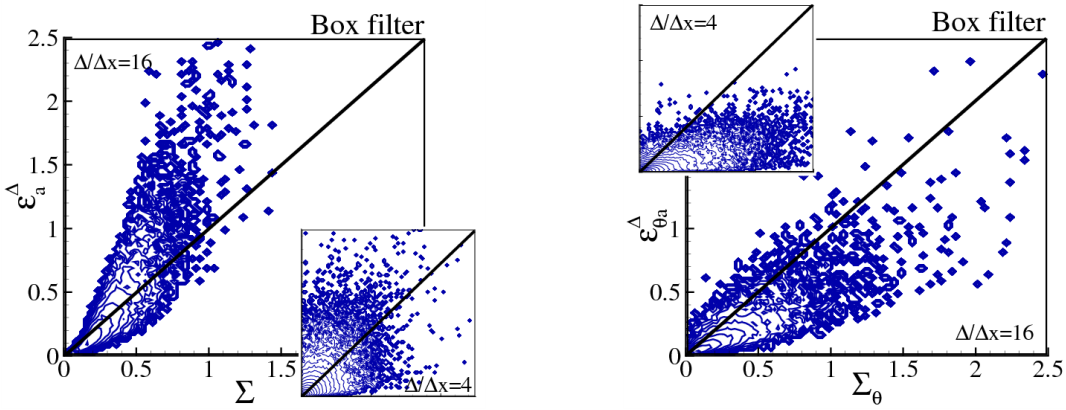

Figure 2: Joint PDFs between (a) the exact (Σ) and modelled (ε_a^Δ) viscous SGS dissipation and; (b) between the exact (Σ_θ) and modelled ($\varepsilon_{\theta a}^\Delta$) molecular SGS dissipation, for the simulations with $Re_\lambda = 95.6$, and $Sc = 0.7$, and for filter widths $\Delta/\Delta x = 4$ and $\Delta/\Delta x = 16$. The classical models for the molecular SGS dissipations ε_a^Δ and $\varepsilon_{\theta a}^\Delta$ are given by equations (5) and (6), respectively.

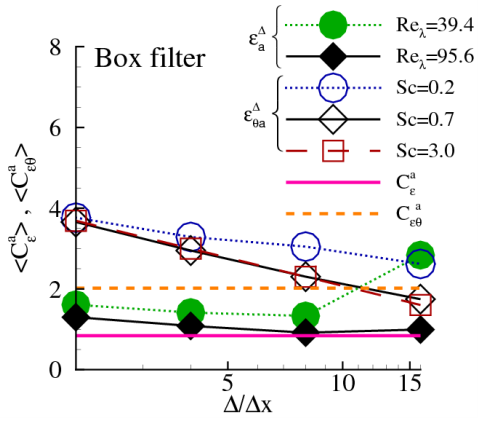

Figure 3: Constants C_ε^a and $C_{\varepsilon\theta}^a$ for all the simulations and filter sizes used in the present work.

is also reasonable, although not as good: no model constant could be chosen in order to obtain a perfect agreement between Σ_θ and $\varepsilon_{\theta a}^\Delta$ for all filter sizes. Moreover, the influence of the Schmidt number is not well reproduced by the model: although the exact molecular SGS dissipation Σ_θ decreases with the Schmidt number, its modelled values $\varepsilon_{\theta a}^\Delta$ increase with Sc.

For the viscous SGS dissipation term we see that the agreement between the skewness factor of the exact Σ and modelled ε_a^Δ quantities is quite good (not shown). Furthermore, the classical model captures again the correct trend in terms of Reynolds number and filter size *i.e.* the skewness of both Σ and ε_a^Δ decreases as the Reynolds number and filter size increases. For the molecular SGS dissipation term again the results are not as good: once more the influence of the Schmidt number is not well captured, even if the skewness of both Σ_θ and $\varepsilon_{\theta a}^\Delta$ seem to be relatively insensitive to changes in the Schmidt number.

The flatness factors for the (exact and modelled) viscous and molecular SGS dissipations terms (not shown) decrease with increasing filter size for all simulations, which indicates a decrease in the intermittency of the dissipation for large filter sizes (as expected) and are again close to the values from da Silva and Métais [12]. However, the results showed again that the classical model ε_a^Δ exhibits the correct trend with the Reynolds number, while $\varepsilon_{\theta a}^\Delta$ does not show the correct trend with the Schmidt number.

Figure 4 (a) and (b) shows the spectra of the exact and modelled viscous/molecular SGS dissipation terms $E_\Sigma(K)$, $E_{\Sigma\theta}(K)$, $E_a(K)$, and $E_{\theta a}(K)$ for filter sizes $\Delta/\Delta x = 4$ and $\Delta/\Delta x = 16$, were each spectra results from averaging over several (10) spectra/instantaneous fields.

Comparing the exact and modelled viscous/molecular SGS dissipations in the Fourier space we see

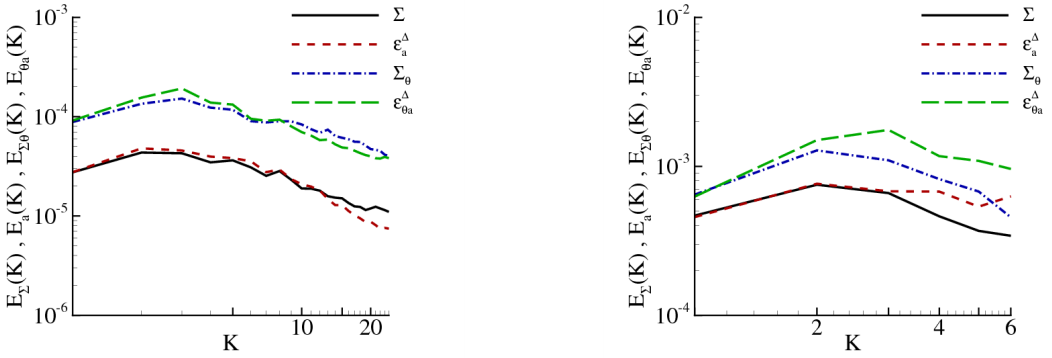

Figure 4: Spectrum of the exact (Σ and Σ_θ) and modelled (ε_a^Δ and $\varepsilon_{\theta a}^\Delta$) molecular SGS dissipation terms for filter widths $\Delta/\Delta x = 4$ (a) and, $\Delta/\Delta x = 16$ (b), for the simulation with $Re_\lambda = 95.6$ and $Sc = 0.7$. Each spectrum results from averaging over several (10) spectra/instantaneous fields, and in order to facilitate the comparison between the exact and modelled spectra the model constants were modified to have $E_\Sigma(K = 0) = E_a(K = 0)$ and $E_{\Sigma\theta}(K = 0) = E_{\theta a}(K = 0)$.

that the agreement between the spectra is generally very good. Moreover, the good agreement between the exact and the modelled spectra exists mainly for small and intermediate wave numbers *i.e.* the differences arise particularly for high wave numbers, where there is more "energy" in the exact than in the modelled viscous/molecular SGS dissipations. Another result that becomes apparent from these plots is that the agreement between the exact and modelled spectra is better for the velocity than for the scalar field. Qualitatively similar results were obtained with the other filter sizes (not shown).

4.2 Analysis of the hybrid RANS/LES models ε_b^Δ and $\varepsilon_{\theta b}^\Delta$

We computed the correlation between the two terms of each side of equations (9) and (10) and confirmed that the local correlation is indeed very small for all the Reynolds and Schmidt numbers and all the filter sizes considered in this work. All the correlation coefficients are displayed in Fig. 5: we obtained $Corr(\Sigma, \varepsilon_b^\Delta) \leqslant 0.16$ and $Corr(\Sigma_\theta, \varepsilon_{\theta b}^\Delta) \leqslant 0.09$. Moreover, the correlations between Σ and ε_b^Δ tend to

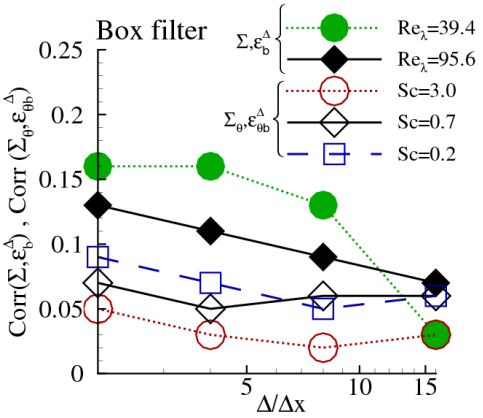

Figure 5: Correlation coefficients between the exact molecular SGS dissipations (Σ and Σ_θ) and their hybrid models (ε_b^Δ and $\varepsilon_{\theta b}^\Delta$) defined by equations (9) and (10). The correlations were obtained with filter widths $\Delta/\Delta x = 2$, 4, 8, and 16, and were computed using the data in the LES mesh.

decrease as the Reynolds number and the filter size increases, while for $Corr(\Sigma_\theta, \varepsilon_{\theta b}^\Delta)$ it is difficult to identify a clear trend on Re_λ, Sc and Δ. Finally, note that the correlations for the dissipation of SGS scalar variance tend to be smaller than those for the SGS kinetic energy equation.

The joint PDF between Σ and ε_b^Δ, and between Σ_θ and $\varepsilon_{\theta b}^\Delta$ are shown in Figs. 6 (a) and (b), respectively. The absence of correlation between the exact and modelled quantities can be observed for

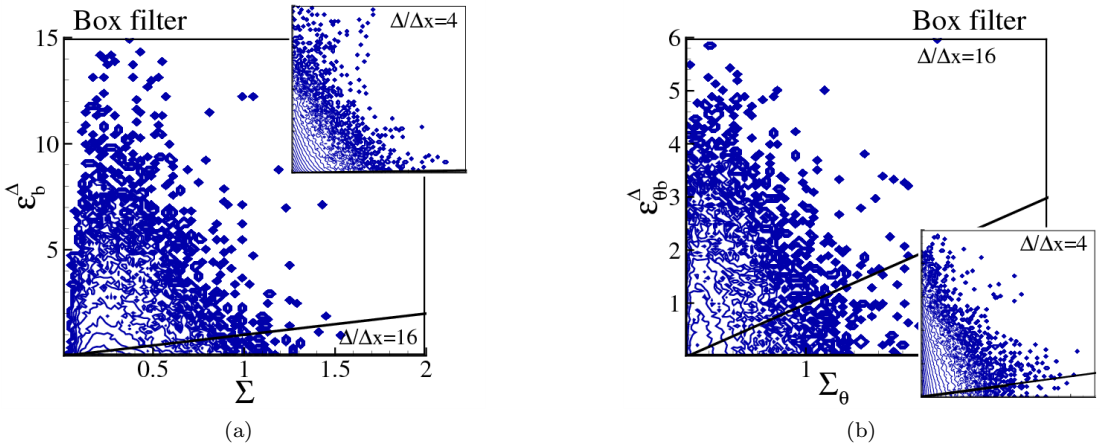

Figure 6: Joint PDFs between (a) the exact (Σ) and modelled (ε_b^Δ) viscous SGS dissipation and; (b) between the exact (Σ_θ) and modelled ($\varepsilon_{\theta b}^\Delta$) molecular SGS dissipation, for the simulations with $Re_\lambda = 95.6$, and $Sc = 0.7$, and for filter widths $\Delta/\Delta x = 4$ and $\Delta/\Delta x = 16$. The hybrid models for the molecular SGS dissipations ε_b^Δ and $\varepsilon_{\theta b}^\Delta$ are given by equations (9) and (10), respectively.

all the range of their values. Note that no discernible difference can be seen between the joint PDFs for $\Delta/\Delta x = 4$ and 16. The same occurs for the other filter sizes (not shown).

Finally, the computation of the model constants $C_{\varepsilon b}^\Delta$ and $C_{\varepsilon\theta b}^\Delta$ defined in equations (9) and (10) was carried out as before. Results are shown in Fig. 7 and show that the values assumed by the constants change by about three orders of magnitude as the filter size varies between $2 \leqslant \Delta/\Delta x \leqslant 16$. Moreover,

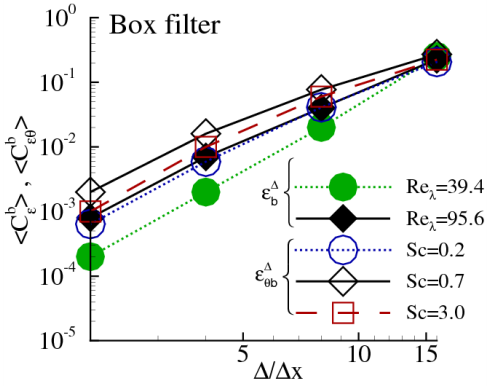

Figure 7: Constants C_ε^b and $C_{\varepsilon\theta}^b$ defined in equations (9) and (10), respectively, for all the simulations and filter sizes used in the present work.

the values of the constants tend to increase dramatically with the filter size, without any tendency to reach an asymptotic value.

The analysis of other one-point statistics such as the variance, skewness and flatness showed also the existence of big differences in terms of statistical characteristics of the exact (Σ and Σ_θ) and modelled (ε_b^Δ and $\varepsilon_{\theta b}^\Delta$) viscous/molecular SGS dissipation terms (not shown). In particular the modelled quantities do not display the correct trend with the filter size *e.g.* the variances of Σ and Σ_θ decreases as the filter size increases, while the modelled variance ε_b^Δ and $\varepsilon_{\theta b}^\Delta$ increase with the filter size. Moreover, the influence of the Reynolds and Schmidt number is not well recovered.

In order to visualise the reason behind these discrepancies between the exact and modelled quantities Fig. 8 shows spectra of the viscous/molecular SGS dissipation terms for all the simulations used in the

present work. Unlike in the classical model discussed before, the spectral shape of the hybrid models for

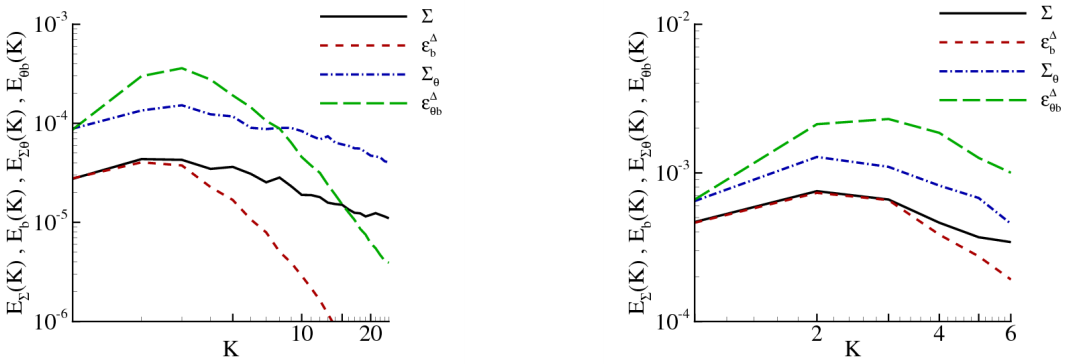

Figure 8: Spectrum of the exact (Σ and Σ_θ) and modelled (ε_b^Δ and $\varepsilon_{\theta b}^\Delta$) molecular SGS dissipation terms for filter widths $\Delta/\Delta x = 4$ (a) and, $\Delta/\Delta x = 16$ (b), for the simulation with $Re_\lambda = 95.6$ and $Sc = 0.7$. Each spectrum results from averaging over several (10) spectra/instantaneous fields, and in order to facilitate the comparison between the exact and modelled spectra the model constants were modified to have $E_\Sigma(K = 0) = E_b(K = 0)$ and $E_{\Sigma\theta}(K = 0) = E_{\theta b}(K = 0)$.

the viscous/molecular SGS dissipation terms defined by equations (9) and (10) is very different from the spectral shape of the real or exact terms.

Furthermore, remark that as with the classical model, the model for the viscous SGS dissipation ε_b^Δ performs better than the model for the molecular SGS dissipation $\varepsilon_{\theta b}^\Delta$.

4.3 Analysis of the model from Jiménez $\varepsilon_{\theta c}^\Delta$

Jiménez *et al.* [5] define a SGS mechanical-to-thermal time scale ratio r_{sgs} (see equation 11), that is invoked in the derivation of the model for ε_c^Δ. Specifically, the model by Jiménez *et al.* [5] implicitly assumes that

$$r_{sgs} \sim \frac{1}{Sc} \tag{16}$$

In order to test this hypothesis r_{sgs} was computed from the present data from its definition given by equation (11). The results are shown in Fig. 9. The values for the (total) mechanical-to-thermal time

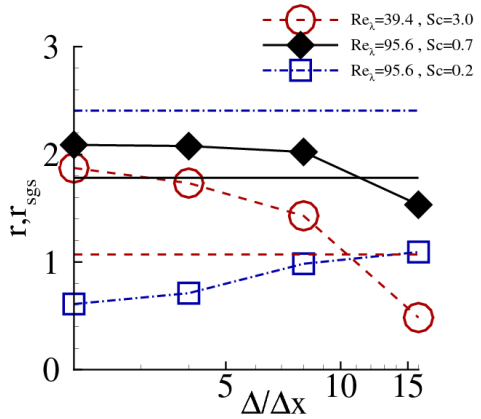

Figure 9: Mechanical-to-thermal time scale ratio defined by equation (12) (lines without symbols), and SGS mechanical-to-thermal time scale ratio defined by equation (11) (lines with symbols) for all the Reynolds and Schmidt numbers and all the filter sizes used in the present work.

scale ratio r defined in equation (12) are also shown.

Starting with r the present results show that r tends to increase with the Reynolds number. Moreover we see that r decreases as the Schmidt number increases. Thus we observe that r is not an universal variable, since it depends on both the Reynolds and Schmidt numbers in agreement with the results from Overholt and Pope [32].

Concerning the SGS mechanical-to-thermal time scale ratio r_{sgs} the results displayed in Fig. 9 show that in addition to its expected dependence on the Reynolds and Schmidt numbers, r_{sgs} varies also with the filter size. The influence of the filter size is difficult to assess with the present data.

We used the present data also to assess whether $r_{sgs} \sim \frac{1}{Sc}$, as supposed by Jiménez *et al.* [5]. As can be seen this is a poor approximation for some cases, while it seems to work reasonably well for others.

The correlation coefficients between the exact (Σ_θ) and modelled ($\varepsilon_{\theta c}$) molecular SGS dissipation using the model by Jiménez *et al.* [5] are shown in Fig. 10 as functions of the Reynolds and Schmidt numbers, and of the filter size for all the simulations used in the present work. As can be seen all

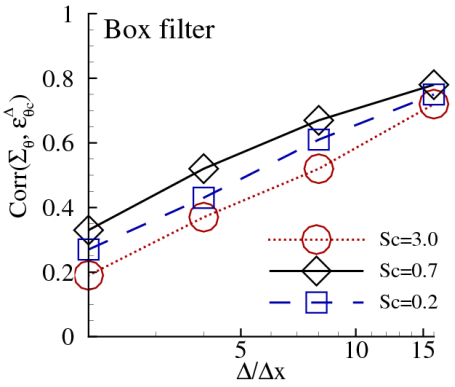

Figure 10: Correlation coefficients between the exact molecular SGS dissipations (Σ_θ) and the model by Jiménez *et al.* [5] ($\varepsilon^{\Delta}_{\theta c}$) defined by equation (14). The correlations were obtained with filter widths $\Delta/\Delta x = 2$, 4, 8, and 16, and were computed using the data in the LES mesh.

the correlations increase fast as the filter size increases, which is a first good indication. Moreover, the correlations are higher for the most important case *i.e.* $Re_\lambda = 95.6$, $Sc = 0.7$ and $\Delta/\Delta x = 16$ (inertial range).

The joint probability density functions (PDFs) between the exact (Σ_θ) and the modelled ($\varepsilon_{\theta c}$) molecular SGS dissipation displayed in Fig. 11 complement the information from the analysis of $Corr(\Sigma_\theta, \varepsilon^{\Delta}_{\theta c})$. For small filter sizes ($\Delta/\Delta x = 4$) there is no correlation between the exact and modelled molecular SGS

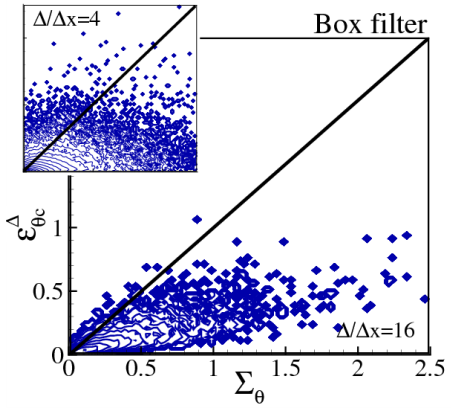

Figure 11: Joint PDFs between the exact (Σ_θ) and modelled ($\varepsilon^{\Delta}_{\theta c}$) molecular SGS dissipation, for the simulations with $Re_\lambda = 95.6$, and $Sc = 0.7$, and for filter widths $\Delta/\Delta x = 4$ and $\Delta/\Delta x = 16$.

dissipation, while for large (inertial range) filter sizes $\Delta/\Delta x = 16$ the correlation is high. The joint probability density functions show also that this high correlation between Σ_θ and $\varepsilon_{\theta c}$ comes from all the range of their values.

The results for the model constant $C^c_{\varepsilon\theta}$ defined by equation (14) are displayed in Fig. 12 and show that the constant assumes values between $0.93 \leqslant C^c_{\varepsilon\theta} \leqslant 5.27$ and show a tendency to increase with the Schmidt number. In contrast with the other models there is no clear trend with the filter size for this

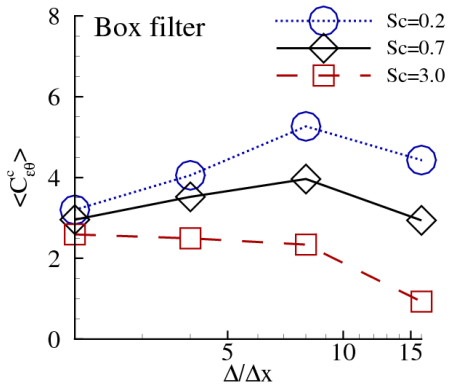

Figure 12: Constant $C^c_{\varepsilon\theta}$ defined in equation (14) for all the simulations and filter sizes used in the present work.

model. Note that the model constant for this model is related with the SGS mechanical-to-thermal scale ratio r_{sgs} through $C^c_{\varepsilon\theta} = 2r_{sgs}$. Therefore we conclude that the determination of the constant $C^c_{\varepsilon\theta}$ in the model from Jiménez *et al.* [5] should be improved for other Schmidt numbers *i.e.* other than $Sc \approx 1.0$.

In order to assess the statistical behaviour of the model $\varepsilon^\Delta_{\theta c}$ we computed the variance, skewness, and flatness of the exact and modelled quantities for all the filter sizes and all the simulations used in this work. As in the classical model the variance of Σ_θ (not shown) is well captured by the model $\varepsilon^\Delta_{\theta c}$ *i.e.* the modelled variance increases with the filter size. In the present case, however, the agreement between the exact and modelled variances is better than in the classical model.

Concerning the skewness factor (not shown) we see that the model from Jiménez *et al.* [5] also provides the correct result of decreasing skewness with increasing filter size, and is generally in good agreement with the exact skewness. For the higher filter sizes (*i.e.* $\Delta/\Delta x = 8$ and $\Delta/\Delta x = 16$) the results are also better than as with the classical model. The same can be said about the evolution of the flatness factor.

To assess the model for the molecular SGS dissipation from Jiménez *et al.* [5] $\varepsilon^\Delta_{\theta c}$ in the wave number space Figs. 13 (a) and (b) show spatial three-dimensional spectra of the exact and modelled molecular SGS dissipation for the simulation with $Re_\lambda = 95.6$ and $Sc = 0.7$, and for filter sizes $\Delta/\Delta x = 4$ and $\Delta/\Delta x = 16$, respectively. As before we denote the spectra of the exact molecular SGS dissipation by $E_{\Sigma\theta}(K)$ while $E_{\theta c}(K)$ represents the spectra of the modelled molecular SGS dissipation. The spectra $E_{\theta a}(K)$ from the classical model is also shown.

By comparing the spectra of the exact and modelled molecular SGS dissipation terms we see that the agreement obtained with the model from Jiménez *et al.* [5] is very good for almost all wave number range. Moreover, note that the results from the model from Jiménez *et al.* [5] are very similar to the results from the classical model *i.e.* $E_{\theta c}(K) \approx E_{\theta a}(K)$, again almost everywhere, except near the end of the wave number range.

5 Conclusions

Using classical *a priori* tests three models for the molecular dissipation of SGS kinetic energy and SGS scalar variance were analysed: (a) the classical model by Yoshizawa [2], (b) the model used in hybrid RANS/LES by *e.g.* Paterson and Peltier [3] and, (c) the model for the molecular SGS dissipation of SGS scalar variance from Jiménez *et al.* [5].

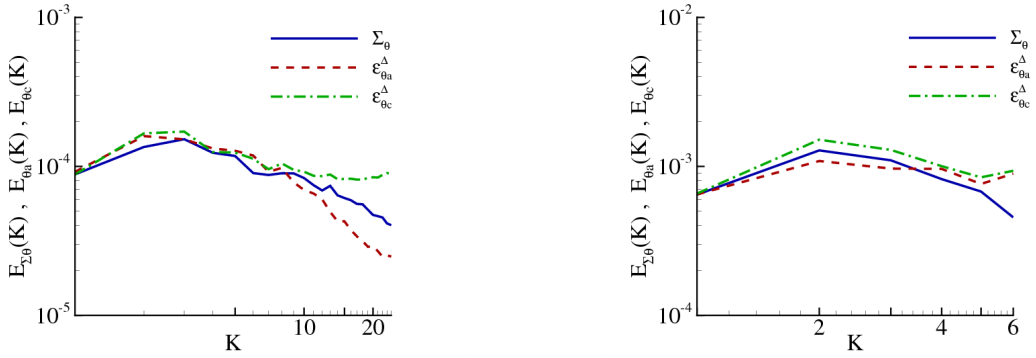

Figure 13: Spectrum of the exact (Σ_θ) and modelled ($\varepsilon^{\Delta}_{\theta c}$) molecular SGS dissipation terms for filter widths $\Delta/\Delta x = 4$ (a) and, $\Delta/\Delta x = 16$ (b), for the simulation with $Re_\lambda = 95.6$ and $Sc = 0.7$. Each spectrum results from averaging over several (10) spectra/instantaneous fields, and in order to facilitate the comparison between the exact and modelled spectra the model constants were modified to have $E_\Sigma(K=0) = E_c(K=0)$ and $E_{\Sigma\theta}(K=0) = E_{\theta c}(K=0)$. Moreover, the spectra for the classical models - $E_a(K)$, $E_{\theta a}(K)$ - is also shown.

Concerning the model constants the results showed that for the classical models the constants tend asymptotically to the theoretical values. For the model by Jiménez *et al.* [5] however, the model constant varies with the Schmidt number in a way which is inconsistent with the approximation $r_{sgs} \sim 1/Sc$ proposed by Jiménez *et al.* [5]. This is a consequence of the lack of Universality of the SGS mechanical-to-thermal time scale ratio r_{sgs}, which is used by several other models. Indeed, in addition to depending - like r the mechanical-to-thermal time scale ratio - on the Reynolds and Schmidt number, r_{sgs} depends also on the size of the implicit grid filter. Therefore a new procedure for the computation of the model constant (at least for Schmidt numbers lower than $Sc \approx 1$) should be pursued. Finally, the model constants used in the hybrid RANS/LES model increase dramatically with the filter size, therefore making it impossible to use them as "constants" during a LES. Moreover, it is unlikely that the dynamic procedure will be able to solve this limitation, and therefore a new methodology for the computation of the model constants must be developed.

Comparison of several one point statistics from the exact and modelled viscous/molecular SGS dissipation terms showed that both classical as well as the model from Jiménez *et al.* [5] give generally good results. For the classical model the results seem to be better for the modelling of Σ than for the modelling of Σ_θ, where the model proposed by Jiménez *et al.* [5] performs even better. On the other hand the results from the hybrid RANS/LES model showed once again very poor results.

The analysis of the exact and modelled viscous/molecular SGS dissipation terms in the Fourier space allowed to explain the main reason behind the poor results displayed by the hybrid RANS/LES model. It turns out that the modelled SGS dissipation given by the hybrid RANS/LES model is concentrated in much lower wave numbers than the exact molecular SGS dissipation, which represents the real trend to be reached.

Thus, the present work demonstrated that the classical model used by Schumann [1] is far superior to the hybrid RANS/LES model from Paterson and Peltier [3]; however, it must be stressed that in some sense this comparison is a bit unfair to the hybrid RANS/LES model since it uses resolved quantities in order to model unresolved quantities, whereas the classical model uses unresolved quantities. In practice the classical model will only be as good as the model used for K_{sgs}.

References

[1] U. Schumann. Subgrid-scale model for finite difference simulations of turbulent flows on plane channels and annuli. *J. Comp. Phys.*, 18:376–404, 1975.

[2] A. Yoshizawa. A statistically-derived subgrid model for the large-eddy simulation of turbulence. *Phys. Fluids*, 25(9):1532–1538, 1982.

[3] E. G. Paterson and L. J. Peltier. Detached-eddy simulation of high-reynolds-number beveled-trailling-edge boundary layers and wakes. *J. Fluids Eng.*, 127:897–906, 2005.

[4] K. Hanjalic. Will rans survive les? a view of perspectives. *Journal of Fluids Engineering*, 127:831–9, 2005.

[5] C. Jiménez, F. Ducros, B. Cuenot, and B. Bédat. Subgrid scale variance and dissipation of a scalar field in large eddy simulations. *Phys. Fluids*, 13(6):1748–1754, 2001.

[6] C.B. da Silva and José C.F. Pereira. Analysis of the gradient-diffusion hypothesis in large-eddy simulations based on transport equations. *Physics of Fluids*, 19:035106, 2007.

[7] M. Lesieur and O. Métais. New trends in large-eddy simulations of turbulence. *Annu. Rev. Fluid Mech.*, 28:45–98, 1999.

[8] C. Meneveau and J. Katz. Scale inveriance and turbulence models for large-eddy simulation. *Annu. Rev. Fluid Mech.*, 32:1–32, 2000.

[9] S. Grag and Z. Warhaft. On the small scale structure of simple shear flow. *Phys. Fluids*, 10:662, 1998.

[10] A. Gilfason and Z. Warhaft. On higher order passive scalar structure functions in grid turbulence. *Phys. Fluids*, 16:4012, 2004.

[11] E. Garnier, O. Métais, and M. Lesieur. Synoptic and Frontal-Cyclone Scale Instabilities in Baroclinic Jet Flows. *J. Atmos. Sci.*, 55:1316–1335, 1998.

[12] C. B. da Silva and O. Métais. On the influence of coherent structures upon interscale interactions in turbulent plane jets. *J. Fluid Mech.*, 473:103–145, 2002.

[13] C. B. da Silva and J. C. F. Pereira. On the local equilibrium of the subgrid-scales: The velocity and scalar fields. *Phys. Fluids*, 17:108103, 2005.

[14] H. Schmidt and U. Schumann. Coherent structure of the convective boundary layer derived from large-eddy simulations. *J. Fluid Mech.*, 200:511–562, 1989.

[15] A. Yoshizawa and K. Horiuti. A statistically-derived subgrid-scale kinetic energy model for the large-eddy simulation of turbulent flows. *J. Phy. Soc. Japan*, 54:2834–2839, 1985.

[16] K. Horiuti. Large-eddy simulation of turbulent channel flow by one-equation modeling. *J. Phy. Soc. Japan*, 54:2855–2865, 1985.

[17] V. C. Wong. A proposed statistical-dynamic closure method for the linear or nonlinear subgrid-scale stresses. *Phys. Fluids*, 4(5):1080–1082, 1992.

[18] S. Ghosal, T. Lund, P. Moin, and K. Akselvol. A dynamic localisation model for large-eddy simulation of turbulent flows. *J. Fluid Mech.*, 286:229–255, 1995.

[19] A. Dejoan and R. Schiestel. Les of unsteady turbulence via a one-equation subgrid-scale transport model. *Int. J. Heat Fluid Flow*, 23:398, 2002.

[20] O. Debliquy, B. Knapen, and D. Carati. A dynamic subgrid-scale model based on the turbulent kinetic energy. In B. J. Geurts, R. Friedrich, and O. Métais, editors, *Direct and large-eddy simulations IV*, pages 89–96. Kluwer Academic Publishers, 2001.

[21] S. Krajnović and L. Davidson. A mixed one equation subgrid model for large-eddy simulation. *Int. J. Heat and Fluid Flow*, 23:413–425, 2002.

[22] R. Schiestel and A. Dejoan. Towards a new partially integrated transport model for coarse grid and unsteady turbulent flow simulations. *Theor. Comput. Fluid. Dyn.*, 18:443, 2005.

[23] L. Davidson and S. Peng. Hybrid les-rans modelling: a one-equation sgs model combined with a $k-w$ model for predicting recirculating flows. *Int. J. Numer. Methods Fluids*, 43:1003–1018, 2003.

[24] C. de Langhe, B. Merci, and E. Dick. Hybrid rans/les modelling with an approximate renormalization group. i: Model development. *Journal of Turbulence*, 6(13), 2005.

[25] C. de Langhe, B. Merci, K. Lodefier, and E. Dick. Hybrid rans/les modelling with an approximate renormalization group. ii: Applications. *Journal of Turbulence*, 6(14), 2005.

[26] T. Kajishima and T. Nomachi. One-equation subgrid scale model using dynamic procedure for the energy dissipation. *J. Appl. Mech., Transactions of ASME*, 73:368–373, 2006.

[27] F. Mathey and J.P. Chollet. Subgrid model of scaler mixing for large-eddy simulation of turbulent flows. In *The Second ERCOFTAC Workshop on Direct and Large-Eddy Simulations, Grenoble, France*, 1996.

[28] Heinz Pitsch. Large-Eddy Simulation of Turbulent Combustion. *Annual Review of Fluid Mechanics*, 38:453–82, 2006.

[29] S. Grimaji and Y. Zhou. Analysis and modeling of subgrid scalar mixing using numerical data. *Phys. Fluids*, 8:1224, 1996.

[30] C. Jiménez, L. Valino, and C. Dopazo. A priori and a posteriori tests of subgrid models for scalar transport. *Phys. Fluids*, 13(8):2433–2436, 2001.

[31] W. Ashusrt et al. Alignment of vorticity and scalar gradient with strain rate in simulated navierstokes turbulence. *Phys. Fluids*, 30:23432353, 1987.

[32] M. Overholt and S. Pope. Direct numerical simulation of a passive scalar with imposed mean gradient in isotropic turbulence. *Phys. Fluids*, 8:31283148, 1996.

[33] P. Vedula, P. Yeung, and R. Fox. Dynamics of scalar dissipation in isotropic turbulence: A numerical and modelling study. *J. Fluid Mech.*, 433:2960, 2001.

[34] J. Schumacher, K. Sreenivasan, and P. Yeung. Very fine structures in scalar mixing. *J. Fluid Mech.*, 531:113122, 2005.

[35] J. Schumacher and K. Sreenivasan. Statistics and geometry of passive scalars in turbulence. *Phys. Fluids*, 17:125107, 2005.

[36] C. Meneveau and J. O'Neil. Scaling laws of the dissipation rate of turbulent subgrid-scale kinetic energy. *Phys. Review E*, 49(4):2866–2874, 1994.

[37] S. Menon, P. K. Yeung, and W. W. Kim. Effect of subgrid models on the computed interscale energy transfer in isotropic turbulence. *Computers and Fluids*, 25(2):165–180, 1996.

[38] S. Chumakov. Scaling properties of subgrid-scale energy dissipation. *Phys. Fluids*, 19:058104, 2007.

[39] C. Pierce and P. Moin. A dynamic model for subgrid-scale variance and dissipation rate of a conserved scalar. *Phys. Fluids*, 12:3041, 1998.

[40] A. Cook and W. Bushe. A subgrid-scale model for the scalar dissipation rate in nonpremixed combustion. *Phys. Fluids*, 11:746, 1999.

[41] B. Chaouat and R. Schiestel. A new partially integrated transport model for subgrid stresses and dissipation rate for turbulent developing flows. *Phys. Fluids*, 17:065106, 2005.

[42] S. Chumakov and C. Rutland. Dynamic structure subgrid-scale models for large eddy simulation. *Int. J. Numer. Methods Fluids*, 47:911–932, 2005.

[43] S. Chumakov and C. Rutland. Dynamic structure models for scalar flux and dissipation in large eddy simulation. *AIAA*, 42:1132–1139, 2004.

[44] U. Piomelli and J. R. Chasnov. Large eddy simulations : Theory and applications. In M. Hall back D. S. Henningson A. V. Jhoannson and P. H. Alfredssoon, editors, *Turbulence and transition modeling*. Kluwer, Dordrecht, 1996.

[45] H. Kang and C. Meneveau. Universality of large eddy simulation parameters across a turbulent wake behind a cylinder heated cylinder. *Journal of Turbulence*, 3(32):1–27, 2002.

[46] H. Tennekes and J. L. Lumley. *A first course in turbulence*. The MIT Press, 1972.

[47] J. Smagorisky. General circulation experiments with the primitive equations. *Mon. Weather Rev.*, 91(3):99–164, 1963.

[48] A. Yoshizawa. Eddy-viscosity-type subgrid-scale model with a variable smagorinsky coefficient and its relationship with the one-equation model in large-eddy simulation. *Phys. Fluids*, 3(8):2007–2009, 1991.

[49] K. Alvelius. Random forcing of three-dimensional homogeneous turbulence. *Phys. Fluids*, 11(7):1880–1889, 1999.

[50] C. B. da Silva, S. Rego, and J. C. F. Pereira. Analysis of the viscous/molecular subgrid-scale dissipation terms in les based on transport equations: A priori tests. *Journal of Turbulence*, 9:1–36, 2008.